*Journal of Sound and Vibration* (2001) **240**(2), 241–262
doi:10.1006/jsvi.2000.3201, available online at http://www.idealibrary.com on IDEAL®

# ACCURATE MODELLING OF A FLEXIBLE-LINK PLANAR MECHANISM BY MEANS OF A LINEARIZED MODEL IN THE STATE-SPACE FORM FOR DESIGN OF A VIBRATION CONTROLLER

A. GASPARETTO

*DIEGM-Dipartimento di Ingegneria Elettrica, Gestionale e Meccanica, Universita di Udine, via delle Scienze*, 208, 1-33100 *Udine, Italy. E-mail: gasparetto@uniud.it*

(*Received* 19 *November* 1999, *and in final form* 2 *June* 2000)

Vibration control of flexible link mechanisms with more than two flexible links is still an open question, mainly because defining a model that is adequate for the designing of a controller is a rather difficult task. In this work, an accurate dynamic non-linear model of a flexible-link planar mechanism is presented. In order to bring the system into a form that is suitable for the design of a vibration controller, the model is then linearized about an operating point, so as to achieve a linear model of the system in the standard state–space form of system theory. The linear model obtained, which is valid for whatever planar mechanism with any number of flexible link, is then applied to a four-bar planar linkage. Extensive simulation is carried out, aimed at comparing the system dynamic evolution, both in the open- and in the closed-loop case, using the non-linear model and the linearized one. The results prove that the error made by using the linearized system instead of the non-linear one is small. Therefore, it can be concluded that the model proposed in this work can constitute an effective basis for designing and testing many types of vibration controllers for flexible planar mechanisms.



## 1. INTRODUCTION

Control of vibration in flexible mechanisms is still an open field for scientific investigation. Although the first investigations were carried out in the early 1970s, the analysis, modelling and control of flexible mechanisms is still very popular, mainly due to the fact that the robot manipulators and automatic mechanisms need to be increasingly lighter and to operate at a higher speed.

Several researchers focused on defining accurate models of flexible mechanisms. Some reviews of the work in this field have been provided by Lowen and Jandrasits [1], Erdman and Sandor [2], Lowen and Chassapis [3] and Book [4]. However, most of the literature turns out to be focused on single-link flexible mechanisms [5–14] or on multi-body systems with only one flexible link [15–18]; in more recent times, some works on two-link flexible planar manipulators are found [19–21]. Among the papers dealing with single-link flexible mechanisms, Giovagnoni [5, 6] presented a mathematical model for a flexible slewing beam subjected to overall large rotation. Bhat *et al.* [7] used the Laplace domain synthesis technique to perform experiments on the precise point-to-point position control of a flexible beam. Cetinkunt and Wu [8] developed a predictive adaptive control algorithm for tip position control of a flexible one arm robot. Kwon and Book [9] solved the inverse dynamic equation of a single-link flexible manipulator in the time domain, in order to

0022-460X/01/070241 + 22 $35.00/0 

calculate the feed-forward torque and the trajectory of all state variables that do not excite structural vibrations for a flexible end-point trajectory. Further work on single-link flexible mechanisms can be found in references [10–14].

Among the papers dealing with multi-body systems with only one flexible link, Hu and Ulsoy [15] used a set of non-linear hybrid ordinary-partial differential equations and an algebraic constraint equation to define a dynamic model for controller design of a constrained rigid–flexible robot arm. Siciliano *et al.* [16] proposed a separate approach for the control of the two subsystems, namely the slow (rigid) one and the fast (flexible) one; an output feedback dynamic compensator is then designed and its optimal gains are computed. Khorrami and Zheng [17] first developed a model based on non-linear partial differential equations to describe the dynamics of a two-link planar manipulator with a flexible forearm; then, they synthesized a controller with an inner loop for the rigid-body motion of the manipulator, and an outer loop for the flexible motion. Yigit [18] designed a PD control for a two-link rigid–flexible manipulator and analyzed its stability.

Among the papers dealing with two-link flexible mechanisms, one can recall the work by Meressi and Paden [19], who investigated the use of robust gain scheduled $H_\infty$ controllers for endpoint trajectory tracking of a two-link flexible manipulator. Xia and Menq [20] proposed an elastic-deformation estimator for real-time end-point tracking control of a flexible two-link manipulator. In a very recent paper, Milford and Asokanthan [21] determined the eigenfrequencies of a two-link flexible manipulator and showed that the eigenfrequencies strongly depend on the manipulator configuration.

As it appears from the above literature review, most of the research in the field is focused on one- or two-link flexible planar manipulators, whereas very little is currently present in the literature regarding the dynamic model and the vibration control of mechanism with more than two flexible links, and particularly closed-chain mechanisms. The main problem in this field of research is to define a suitable model of the mechanism, which must be accurate enough to represent effectively the real system, but simple enough to enable one to use such a model to implement an effective vibration control. Models of flexible multi-body systems were proposed by Nagarajan and Turcic [22, 23], who used a Lagrangian formulation, and by Meirovitch and Stemple [24], who formulated the dynamics of a flexible system by means of a set of hybrid (ordinary and partial) differential equations of motion in terms of quasi-co-ordinates. Lieh [25] introduced a method leading to separated-form formulation of dynamic equations of multi-body systems subject to control. Yang and Park [26] presented a stability analysis method for a closed-loop flexible mechanism. One of the few applications of a control of a four-bar mechanism (with a flexible coupler link) can be found in a very recent paper by Karkoub and Yigit [27].

In this paper an accurate dynamic model of a flexible-link planar mechanism, which constitutes the basis to develop any compensator for vibration control, is presented. The mechanism links are modelled by beam elements according to the finite elements method. The overall motion of the mechanism is decomposed into the rigid motion of a suitably defined equivalent rigid link mechanism (ERLS) and an overlapped elastic motion, following the ideas set forward by Turcic and Midha [28–30], Chang and Hamilton [31] and Giovagnoni [32]. The equations of motion for the flexible mechanism can then be written by direct application of the virtual work principle. In this way, a system of equations is obtained which provides the elastic accelerations of the nodes as well as the accelerations of the free co-ordinates of the mechanism. The corresponding velocities and displacements can then be computed by integration.

However, such a model is strongly non-linear due to the quadratic relation between the nodal accelerations and the velocities of the free co-ordinates. In order to get a model of the system in the standard state-space form of system theory, it is necessary to linearize the

model about an operating point. The linearization of the non-linear model of any flexible-link planar mechanism is presented, and then applied to the case of a four-bar planar linkage. The validity of the linearization has been checked by comparing the output of the linearized model with the output of the non-linear one. It is shown that the difference between the two results, i.e., the error introduced by the linearization, is small. This proves the effectiveness of the linearization for a rather large interval centered at the operating point; hence, the linearized model is definitely effective to represent the system in a state-space form. This will enable one to implement whatever state-space control (for instance, an optimal control) of the vibrations of a flexible mechanism.

## 2. DYNAMIC MODEL OF A FLEXIBLE-LINK MECHANISM

The dynamic model of a flexible-link mechanism used in this work is based on the theory proposed by Giovagnoni [32] and is summarized here. The accuracy of such a model has been proved by experimental tests, the results of which are presented in the same paper [32]. Each flexible link of the mechanism is subdivided into finite elements, and an ERLS is defined so that the elastic displacements with respect to it can be considered. Figure 1 shows the main entities used in the model.

The following definitions are made, with respect to a fixed reference frame $\{X, Y, Z\}$: $\mathbf{u}_i$ is the nodal displacement vector for the $i$th finite element; $\mathbf{r}_i$ is the nodal position vector for the $i$th element of the ERLS; $\mathbf{b}_i$ is the nodal position vector for the $i$th finite element, given by the sum of the nodal elastic displacements and of the ERLS position:

$$\mathbf{b}_i = \mathbf{r}_i + \mathbf{u}_i, \tag{1}$$

where $\mathbf{v}_i$ is the elastic displacement vector of a generic point inside the $i$th element; $\mathbf{w}_i$ is the position vector of the generic point of the $i$th element of the ERLS; $\mathbf{p}_i$ is the position vector of the generic point of the $i$th finite element, given by the sum of the position of the point in the ERLS and of its elastic displacement:

$$\mathbf{p}_i = \mathbf{w}_i + \mathbf{v}_i. \tag{2}$$

As stated in the foregoing, all the above vectors are measured in a fixed reference frame $\{X, Y, Z\}$. However, for each finite element a local co-ordinate system $\{x_i, y_i, z_i\}$ is defined, which follows the ERLS motion. Thus, a block-diagonal global-to-local transformation matrix $\mathbf{T}_i(\mathbf{q})$ as well as a local-to-global transformation matrix $\mathbf{R}_i(\mathbf{q})$ are to be defined. In

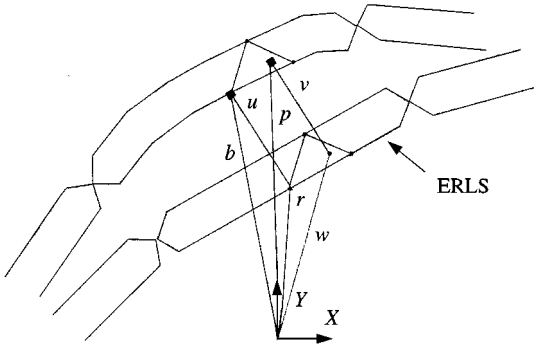


Figure 1. Model of the mechanism.

this way, equation (2) can be rewritten as

$$\mathbf{p}_i = \mathbf{w}_i + \mathbf{R}_i(\mathbf{q})\mathbf{N}_i(x_i, y_i, z_i)\mathbf{T}_i(\mathbf{q})\mathbf{u}_i, \tag{3}$$

where $\mathbf{N}_i(x_i, y_i, z_i)$ is the shape function matrix for the interpolation of the $i$th finite element defined in the local frame.

For the virtual displacements which are to be used in the application of the virtual work principle one can write

$$\delta\mathbf{p}_i = \delta\mathbf{w}_i + \delta\mathbf{v}_i, \tag{4}$$

where the first term on the right-hand side is expressed by

$$\delta\mathbf{w}_i = \mathbf{R}_i(\mathbf{q})\mathbf{N}_i(x_i, y_i, z_i)\mathbf{T}_i(\mathbf{q})\delta\mathbf{r}_i, \tag{5}$$

and the second virtual term on the right-hand side of $\delta\mathbf{v}_i$ in equation ((4)) is obtained by considering both virtual nodal displacements $\delta\mathbf{u}_i$ and virtual displacements $\delta\mathbf{q}$ of the generalized co-ordinates. In this way, the expression for the virtual displacements in the fixed reference frame becomes

$$\begin{aligned}\delta\mathbf{p}_i = {} & \mathbf{R}_i(\mathbf{q})\mathbf{N}_i(x_i, y_i, z_i)\mathbf{T}_i(\mathbf{q})\delta\mathbf{r}_i + \delta\mathbf{R}_i(\mathbf{q})\mathbf{N}_i(x_i, y_i, z_i)\mathbf{T}_i(\mathbf{q})\mathbf{u}_i \\ & + \mathbf{R}_i(\mathbf{q})\mathbf{N}_i(x_i, y_i, z_i)\delta\mathbf{T}_i(\mathbf{q})\mathbf{u}_i + \mathbf{R}_i(\mathbf{q})\mathbf{N}_i(x_i, y_i, z_i)\mathbf{T}_i(\mathbf{q})\delta\mathbf{u}_i.\end{aligned} \tag{6}$$

Equation (6) can be simplified if terms of lower order of magnitude are neglected, thus obtaining the expression

$$\delta\mathbf{p}_i = \mathbf{R}_i\mathbf{N}_i(x_i, y_i, z_i)\mathbf{T}_i\delta\mathbf{r}_i + \mathbf{R}_i\mathbf{N}_i(x_i, y_i, z_i)\mathbf{T}_i\delta\mathbf{u}_i. \tag{7}$$

Differentiating equation (3) twice yields the expression of the acceleration of a generic point inside the $i$th finite element:

$$\begin{aligned}\ddot{\mathbf{p}}_i = {} & \mathbf{R}_i(\mathbf{q})\mathbf{N}_i(x_i, y_i, z_i)\mathbf{T}_i(\mathbf{q})\ddot{\mathbf{r}}_i + \mathbf{R}_i(\mathbf{q})\mathbf{N}_i(x_i, y_i, z_i)\mathbf{T}_i(\mathbf{q})\ddot{\mathbf{u}}_i \\ & + 2(\dot{\mathbf{R}}_i(\mathbf{q})\mathbf{N}_i(x_i, y_i, z_i)\mathbf{T}_i(\mathbf{q}) + \mathbf{R}_i(\mathbf{q})\mathbf{N}_i(x_i, y_i, z_i)\dot{\mathbf{T}}_i(\mathbf{q}))\dot{\mathbf{u}}_i \\ & + (\ddot{\mathbf{R}}_i(\mathbf{q})\mathbf{N}_i(x_i, y_i, z_i)\mathbf{T}_i(\mathbf{q}) + 2\dot{\mathbf{R}}_i(\mathbf{q})\mathbf{N}_i(x_i, y_i, z_i)\dot{\mathbf{T}}_i(\mathbf{q}) \\ & + \mathbf{R}_i(\mathbf{q})\mathbf{N}_i(x_i, y_i, z_i)\ddot{\mathbf{T}}_i(\mathbf{q}))\mathbf{u}_i.\end{aligned} \tag{8}$$

Again, by neglecting terms of lower order of magnitude, one gets a simplified expression

$$\begin{aligned}\ddot{\mathbf{p}} = {} & \mathbf{R}_i\mathbf{N}_i(x_i, y_i, z_i)\mathbf{T}_i\ddot{\mathbf{r}}_i + \mathbf{R}_i\mathbf{N}_i(x_i, y_i, z_i)\mathbf{T}_i\ddot{\mathbf{u}}_i + 2(\dot{\mathbf{R}}_i\mathbf{N}_i(x_i, y_i, z_i)\mathbf{T}_i \\ & + \mathbf{R}_i\mathbf{N}_i(x_i, y_i, z_i)\dot{\mathbf{T}}_i)\dot{\mathbf{u}}_i.\end{aligned} \tag{9}$$

A further insight into the kinematics of the system should now be done. If the kinematic entities of all the finite elements are grouped into a unique vector, equation (1) becomes, after differentiation,

$$\mathrm{d}\mathbf{b} = \mathrm{d}\mathbf{u} + \mathrm{d}\mathbf{r}. \tag{10}$$

The configuration of the ERLS (as well as its velocity and acceleration) depends uniquely on the vector $\mathbf{q}$ of the free co-ordinates; this can be mathematically expressed as

$$\mathrm{d}\mathbf{r} = \mathbf{S}(\mathbf{q})\,\mathrm{d}\mathbf{q}, \quad \dot{\mathbf{r}} = \mathbf{S}(\mathbf{q})\dot{\mathbf{q}}, \tag{11, 12}$$

$$\ddot{\mathbf{r}} = \mathbf{S}(\mathbf{q})\ddot{\mathbf{q}} + \dot{\mathbf{S}}(\mathbf{q}, \dot{\mathbf{q}})\dot{\mathbf{q}} = \mathbf{S}(\mathbf{q})\ddot{\mathbf{q}} + \left(\sum_k \dot{q}_k \frac{\partial \mathbf{S}}{\partial q_k}\right)\dot{\mathbf{q}}, \tag{13}$$

where $\mathbf{S}(\mathbf{q})$ is the matrix of the sensitivity coefficients for all the nodes. This matrix is an explicit function of the $\mathbf{q}$ vector, and its columns contain the nodal rigid-body velocities corresponding to unit velocities of the generalized co-ordinates of the ERLS.

Then, by substituting equation (11) into equation (10), and setting the expression in matrix form, one obtains

$$\mathrm{d}\mathbf{b} = [\mathbf{I}\,|\,\mathbf{S}]\begin{bmatrix}\mathrm{d}\mathbf{u} \\ \hdashline \mathrm{d}\mathbf{q}\end{bmatrix}. \tag{14}$$

The coefficient matrix of equation (14) is not square; hence, a given configuration $\mathrm{d}\mathbf{b}$ of infinitesimal nodal displacements corresponds to more sets of increments $\lfloor\, \mathrm{d}\mathbf{u}^{(\mathrm{T})}\,|\,\mathrm{d}\mathbf{q}^{\mathrm{T}}\,\rfloor$ of the generalized co-ordinates of the system. The easiest way to eliminate this redundancy is to force to zero a number of elements of $\mathrm{d}\mathbf{u}$ equal to the number of generalized co-ordinates of the ERLS. If $\mathrm{d}\mathbf{u}$ is partitioned into its independent part ($\mathrm{d}\mathbf{u}_{in}$) and into its zeroed part ($\mathrm{d}\mathbf{u}_0$), and if $\mathbf{S}$ is correspondingly partitioned,the element forced to zero can be eliminated from equation (14):

$$\mathrm{d}\mathbf{b} = \begin{bmatrix}\mathbf{I} & \mathbf{S}_{in} \\ \hdashline 0 & \mathbf{S}_0\end{bmatrix}\begin{bmatrix}\mathrm{d}\mathbf{u}_{in} \\ \hdashline \mathrm{d}\mathbf{q}\end{bmatrix} \tag{15}$$

The square matrix of coefficients of equation (15) must be non-singular, which implies that the determinant of $\mathbf{S}_0$ must be different from zero; moreover, a correct ERLS definition requires the generalized co-ordinates of the ERLS to be chosen in a way that no singular configuration is encountered during the motion.

Once these kinematic definitions have been set, the dynamic equations of motion for the flexible mechanism can be obtained by applying the principle of virtual work:

$$\delta W^{inertia} + \delta W^{elastic} + \delta W^{external} = 0. \tag{16}$$

A more explicit definition of equation (16) is given by

$$\underbrace{\sum_i \int_{v_i} \mathbf{P}_i^{\mathrm{T}} \ddot{\mathbf{p}}_i \rho_i \,\mathrm{d}v}_{\delta W^{inertia}} + \underbrace{\sum_i \int_{v_i} \delta\varepsilon_i^{\mathrm{T}} \mathbf{D}_i \varepsilon_i \,\mathrm{d}v}_{\delta W^{elastic}} = \underbrace{\sum_i \int_{v_i} \delta\mathbf{p}_i^{\mathrm{T}} \mathbf{g} \rho_i \,\mathrm{d}v + (\delta\mathbf{u}^{\mathrm{T}} + \delta\mathbf{r}^{\mathrm{T}})\,\mathbf{f}}_{-\delta W^{external}}, \tag{17}$$

where $\mathbf{D}_i$, $\varepsilon_i$ and $\rho_i$ are, respectively, the stress–strain matrix, the strain vector and the mass density for the $i$th element, $\mathbf{g}$ is the gravity acceleration vector, and $\mathbf{f}$ is the vector of the concentrated external forces and torques. The total virtual work is split into the integrals over element volumes $v_i$ and in the virtual work due to $\mathbf{f}$, $\delta\mathbf{u}$ and $\delta\mathbf{r}$ refer to all the nodes of the model.

Now, by considering equations (6) and (8), and by introducing the following definitions:

$$\int_{v_i} \mathbf{T}_i^{\mathrm{T}} \mathbf{N}_i^{\mathrm{T}} \mathbf{R}_i^{\mathrm{T}} \mathbf{R}_i \mathbf{N}_i \mathbf{T}_i \rho_i \, \mathrm{d}v = \mathbf{M}_i, \quad \int_{v_i} T_i^{\mathrm{T}} \mathbf{B}_i^{\mathrm{T}} \mathbf{D}_i \mathbf{B}_i \mathbf{T}_i \, \mathrm{d}v = \mathbf{K}_i, \quad \int_{v_i} \mathbf{T}_i^{\mathrm{T}} \mathbf{N}_i^{\mathrm{T}} \mathbf{R}_i^{\mathrm{T}} \mathbf{g} \rho_i \, \mathrm{d}v = \mathbf{f}_g, \tag{18–20}$$

$$\int_{v_i} \mathbf{T}_i^{\mathrm{T}} \mathbf{N}_i^{\mathrm{T}} \mathbf{R}_i^{\mathrm{T}} \dot{\mathbf{R}}_i \mathbf{N}_i \mathbf{T}_i \rho_i \, \mathrm{d}v = \mathbf{M}_{G1i}, \quad \int_{v_i} \mathbf{T}_i^{\mathrm{T}} \mathbf{N}_i^{\mathrm{T}} \mathbf{R}_i^{\mathrm{T}} \mathbf{R}_i \mathbf{N}_i \dot{\mathbf{T}}_i \rho_i \, \mathrm{d}v = \mathbf{M}_{G2i}, \quad \delta \mathbf{T}_i^{\mathrm{T}} = \delta \phi_i \mathbf{T}_i^{\mathrm{T}}, \tag{21–23}$$

Equation (17) can be rearranged in the form

$$\begin{aligned} \sum_i \delta \mathbf{u}_i^{\mathrm{T}} \mathbf{M}_i (\ddot{\mathbf{r}}_i + \ddot{\mathbf{u}}_i) + 2 \sum_i \delta \mathbf{u}_i^{\mathrm{T}} (\mathbf{M}_{G1i} + \mathbf{M}_{G2i}) \dot{\mathbf{u}}_i + \sum_i \delta \mathbf{r}_i^{\mathrm{T}} \mathbf{M}_i (\ddot{\mathbf{r}}_i + \ddot{\mathbf{u}}_i) \\ + 2 \sum_i \delta \mathbf{r}_i^{\mathrm{T}} (\mathbf{M}_{G1i} + \mathbf{M}_{G2i}) \dot{\mathbf{u}}_i + \sum_i \delta \mathbf{u}_i^{\mathrm{T}} \mathbf{K}_i \mathbf{u}_i + \sum_i \mathbf{u}_i^{\mathrm{T}} \delta \phi_i \mathbf{K}_i \mathbf{u}_i \\ = \sum_i (\delta \mathbf{u}_i^{\mathrm{T}} + \delta \mathbf{r}_i^{\mathrm{T}}) \mathbf{f}_{gi} + (\delta \mathbf{u}^{\mathrm{T}} + \delta \mathbf{r}^{\mathrm{T}}) \mathbf{f}. \end{aligned} \tag{24}$$

A more detailed explanation is contained in reference [32]. Now, nodal elastic virtual displacements $\delta \mathbf{u}$ and virtual displacements of the ERLS $\delta \mathbf{r}$ are completely independent with each other. Hence, equation (24) can be subdivided into two equations

$$\delta \mathbf{u}^{\mathrm{T}} \mathbf{M} (\ddot{\mathbf{r}} + \ddot{\mathbf{u}}) + 2 \delta \mathbf{u}^{\mathrm{T}} \mathbf{M}_G \dot{\mathbf{u}} + \delta \mathbf{u}^{\mathrm{T}} \mathbf{K} \mathbf{u} = \delta \mathbf{u}^{\mathrm{T}} (\mathbf{f}_g + \mathbf{f}), \tag{25}$$

$$\delta \mathbf{r}^{\mathrm{T}} \mathbf{M} (\ddot{\mathbf{r}} + \ddot{\mathbf{u}}) + 2 \delta \mathbf{r}^{\mathrm{T}} \mathbf{M}_G \dot{\mathbf{u}} = \delta \mathbf{r}^{\mathrm{T}} (\mathbf{f}_g + \mathbf{f}), \tag{26}$$

where $\mathbf{M}$ is the mass matrix, $\mathbf{M}_G = \mathbf{M}_{G1} + \mathbf{M}_{G2}$ the Coriolis matrix, $\mathbf{K}$ the stiffness matrix of the mechanism, $\mathbf{f}_g$ is the gravity force vector and $\mathbf{f}$ the vector of the external loads applied to the mechanism.

Equation (25) is a statement that nodal equilibrium: equivalent loads applied to each node must be in equilibrium. Equation (26) is the statement of overall equilibrium of all equivalent nodal loads applied to the linkage produce no work for virtual displacement of the ERLS.

Now, the infinitesimal displacements of the ERLS can be expressed by means of the sensitivity coefficient matrix, as in equation (11), and the $\delta \mathbf{u}$'s and the $\delta \mathbf{r}$'s can be eliminated from equations (25) and (26) respectively. Hence, the following system of differential equations is obtained:

$$\mathbf{M} (\ddot{\mathbf{r}} + \ddot{\mathbf{u}}) + 2 \mathbf{M}_G \dot{\mathbf{u}} + \mathbf{K} \mathbf{u} = (\mathbf{f}_g + \mathbf{f}), \tag{27}$$

$$\mathbf{S}^{\mathrm{T}} \mathbf{M} (\ddot{\mathbf{r}} + \ddot{\mathbf{u}}) + 2 \mathbf{S}^{\mathrm{T}} \mathbf{M}_G \dot{\mathbf{u}} = \mathbf{S}^{\mathrm{T}} (\mathbf{f}_g + \mathbf{f}). \tag{28}$$

Practical applications need some damping to be introduced. If simple Rayleigh damping is introduced, equations (27) and (28) become

$$\mathbf{M} (\ddot{\mathbf{r}} + \ddot{\mathbf{u}}) + 2 \mathbf{M}_G \dot{\mathbf{u}} + \alpha \mathbf{M} \dot{\mathbf{u}} + \beta \mathbf{K} \dot{\mathbf{u}} + \mathbf{K} \mathbf{u} = (\mathbf{f}_g + \mathbf{f}), \tag{29}$$

$$\mathbf{S}^{\mathrm{T}} \mathbf{M} (\ddot{\mathbf{r}} + \ddot{\mathbf{u}}) + 2 \mathbf{S}^{\mathrm{T}} \mathbf{M}_G \dot{\mathbf{u}} + \alpha \mathbf{S}^{\mathrm{T}} \mathbf{M} \dot{\mathbf{u}} = \mathbf{S}^{\mathrm{T}} (\mathbf{f}_g + \mathbf{f}). \tag{30}$$

In order to get an explicit integration scheme, equations (29) and (30) can be rearranged in matrix form

$$\begin{bmatrix} \mathbf{M} & \mathbf{MS} \\ \mathbf{S}^{\mathrm{T}}\mathbf{M} & \mathbf{S}^{\mathrm{T}}\mathbf{MS} \end{bmatrix} \begin{bmatrix} \ddot{\mathbf{u}} \\ \ddot{\mathbf{q}} \end{bmatrix} = \begin{bmatrix} \mathbf{t}(\mathbf{u}, \dot{\mathbf{u}}, \mathbf{q}, \dot{\mathbf{q}}) \\ \mathbf{S}^{\mathrm{T}}\mathbf{t}(\mathbf{u}, \dot{\mathbf{u}}, \mathbf{q}, \dot{\mathbf{q}}) \end{bmatrix}. \tag{31}$$

In this way, the values of the accelerations can be computed at each step by solving the system (20), while the values of velocities and of displacements can be obtained by an appropriate integration scheme (e.g., the Runge–Kutta algorithm).

## 3. LINEARIZATION OF THE MODEL

An important step in the study of the dynamics of a flexible mechanism was to bring the above model into the state-space form. In this way, the methods of system theory could be applied to the model. According to the theory, the state-space form expressing the temporal evolution of a generic dynamic system is given by

$$\dot{\mathbf{x}}(t) = \mathbf{f}(\mathbf{x}(t), \mathbf{v}(t)), \quad \mathbf{y}(t) = \mathbf{h}(\mathbf{x}(t), \mathbf{v}(t)), \tag{32}$$

where $\mathbf{x}$ is the state vector, $\mathbf{v}$ is the input vector, $\mathbf{y}$ is the output vector and $\mathbf{f}$ and $\mathbf{h}$ are the system functions.

System theory often considers the standard state-space form of a linear, time-invariant dynamic system, that is expressed by

$$\dot{\mathbf{x}}(t) = \mathbf{F}\mathbf{x}(t) + \mathbf{G}\mathbf{v}(t), \quad \mathbf{y}(t) = \mathbf{H}\mathbf{x}(t) + \mathbf{D}\mathbf{v}(t), \tag{33}$$

where the matrices, $\mathbf{F}$, $\mathbf{G}$, $\mathbf{H}$ and $\mathbf{D}$ are not dependent on time.

In order to bring the system under investigation into the state-space form, equations (29) and (30) are rewritten in matrix form, yielding

$$\begin{bmatrix} \mathbf{M} & \mathbf{MS} \\ \mathbf{S}^{\mathrm{T}}\mathbf{M} & \mathbf{S}^{\mathrm{T}}\mathbf{MS} \end{bmatrix} * \begin{bmatrix} \ddot{\mathbf{u}} \\ \ddot{\mathbf{q}} \end{bmatrix} = \begin{bmatrix} -2\mathbf{M}_G - \alpha\mathbf{M} - \beta\mathbf{K} & -\mathbf{M}\dot{\mathbf{S}} & -\mathbf{K} \\ \mathbf{S}^{\mathrm{T}}(-2\mathbf{M}_G - \alpha\mathbf{M}) & -\mathbf{S}^{\mathrm{T}}\mathbf{M}\dot{\mathbf{S}} & \mathbf{0} \end{bmatrix} * \begin{bmatrix} \dot{\mathbf{u}} \\ \dot{\mathbf{q}} \\ \mathbf{u} \end{bmatrix}$$

$$+ \begin{bmatrix} \mathbf{M} & \mathbf{I} \\ \mathbf{S}^{\mathrm{T}}\mathbf{M} & \mathbf{S}^{\mathrm{T}} \end{bmatrix} * \begin{bmatrix} \mathbf{g} \\ \mathbf{f} \end{bmatrix}. \tag{34}$$

Then, taking $\mathbf{x} = [\dot{\mathbf{u}}\ \ \dot{\mathbf{q}}\ \ \mathbf{u}\ \ \mathbf{q}]^{\mathrm{T}}$ as the augmented state vector, and rearranging the matrices, the system expressing the dynamics of the mechanism can be written as

$$\begin{bmatrix} \mathbf{M} & \mathbf{MS} & \mathbf{0} & \mathbf{0} \\ \mathbf{S}^{\mathrm{T}}\mathbf{M} & \mathbf{S}^{\mathrm{T}}\mathbf{MS} & \mathbf{0} & \mathbf{0} \\ \mathbf{0} & \mathbf{0} & \mathbf{I} & \mathbf{0} \\ \mathbf{0} & \mathbf{0} & \mathbf{0} & \mathbf{I} \end{bmatrix} \begin{bmatrix} \ddot{\mathbf{u}} \\ \ddot{\mathbf{q}} \\ \dot{\mathbf{u}} \\ \dot{\mathbf{q}} \end{bmatrix} = \begin{bmatrix} -2\mathbf{M}_G - \alpha\mathbf{M} - \beta\mathbf{K} & -\mathbf{M}\dot{\mathbf{S}} & -\mathbf{K} & \mathbf{0} \\ \mathbf{S}^{\mathrm{T}}(-2\mathbf{M}_G - \alpha\mathbf{M}) & \mathbf{S}^{\mathrm{T}}\mathbf{MS} & \mathbf{0} & \mathbf{0} \\ \mathbf{I} & \mathbf{0} & \mathbf{0} & \mathbf{0} \\ \mathbf{0} & \mathbf{I} & \mathbf{0} & \mathbf{0} \end{bmatrix} \begin{bmatrix} \dot{\mathbf{u}} \\ \dot{\mathbf{q}} \\ \mathbf{u} \\ \mathbf{q} \end{bmatrix}$$

$$+ \begin{bmatrix} \mathbf{M} & \mathbf{I} \\ \mathbf{S}^{\mathrm{T}}\mathbf{M} & \mathbf{S}^{\mathrm{T}} \\ \mathbf{0} & \mathbf{0} \\ \mathbf{0} & \mathbf{0} \end{bmatrix} \begin{bmatrix} \mathbf{g} \\ \mathbf{f} \end{bmatrix}. \tag{35}$$

Equation (35) can be rewritten in a more compact form

$$\mathbf{A}(\mathbf{x}(t))\dot{\mathbf{x}}(t) = \mathbf{B}(\mathbf{x}(t))\mathbf{x}(t) + \mathbf{C}(\mathbf{x}(t))\mathbf{v}(t), \tag{36}$$

where it should be noted that the **A**, **B** and **C** matrices do not depend on the input vector **v**.

System (35) is non-linear, because the $\dot{\mathbf{S}}$ matrix contains the values of the velocities $\dot{\mathbf{q}}$ of the free co-ordinates (i.e., $\dot{\mathbf{S}} = \dot{\mathbf{S}}(\mathbf{q}, \dot{\mathbf{q}})$), which yields a quadratic term $\dot{\mathbf{q}}^2$ in the velocities of the free co-ordinates, as expressed by equation (13). It is now required to linearize the non-linear system (35) about an equilibrium point $\mathbf{x}_e$, $\mathbf{v}_e$, i.e., a point for which, recalling equation (32), $\dot{\mathbf{x}}_e = \mathbf{f}(\mathbf{x}_e, \mathbf{v}_e) = \mathbf{0}$.

A linearization procedure will now be applied. For generic vectors $\mathbf{x}(t)$, $\mathbf{v}(t)$ near the operating point one can write $\mathbf{x}(t) = \mathbf{x}_e + \Delta\mathbf{x}(t)$, $\mathbf{v}(t) + \mathbf{v}_e + \Delta\mathbf{x}(t)$. Then, introducing such expressions into equation ((23)) yields

$$\mathbf{A}(\mathbf{x}_e + \Delta\mathbf{x}(t))(\dot{\mathbf{x}}_e + \Delta\dot{\mathbf{x}}(t)) = \mathbf{B}(\mathbf{x}_e + \Delta\mathbf{x}(t))(\mathbf{x}_e + \Delta x(t)) + \mathbf{C}(\mathbf{x}_e + \Delta\mathbf{x}(t))(\mathbf{v}_e + \Delta\mathbf{v}(t)). \tag{37}$$

Now, one can get the exact expressions for the terms appearing in equation (37). Considering the $i$th row on the left-hand side of equation (37), and recalling that $\dot{\mathbf{x}}_e = \mathbf{0}$,

$$\begin{aligned}
&\sum_{j=1}^{n} A_{i,j}(x_{e1} + \Delta x_1, x_{e2} + \Delta x_2, \ldots, x_{en} + \Delta x_n) * \Delta\dot{x}_j \\
&\quad = \sum_{j=1}^{n} A_{i,j}(x_{e1}, x_{e2}, \ldots, x_{en}) * \Delta\dot{x}_j + \sum_{k=1}^{n}\left[\sum_{j=1}^{n} \left.\frac{\partial A_{i,j}}{\partial x_k}\right|_{x=x_e} \Delta x_k\, \Delta\dot{x}_j\right] \\
&\quad = \sum_{j=1}^{n} A_{i,j}(x_{e1}, x_{e2}, \ldots, x_{en}) * \Delta\dot{x}_j,
\end{aligned} \tag{38}$$

where the higher order term $\sum_{k=1}^{n}[\sum_{j=1}^{n} \partial A_{i,j}/\partial x_k|_{x=x_e}\, \Delta x_k \Delta\dot{x}_j]$ can be neglected.

Now, by applying similar considerations on the right-hand side of equation (37), for the first term one obtains

$$\begin{aligned}
&\sum_{j=1}^{n} B_{i,j}(x_{e1} + \Delta x_1, x_{e2} + \Delta x_2, \ldots, x_{en} + \Delta x_n) * (v_{ez} + \Delta x_j) \\
&\quad = \sum_{j=1}^{n} B_{i,j}(x_{e1}, x_{e2}, \ldots, x_{en}) * x_{ej} + \sum_{j=1}^{n} B_{i,j}(x_{e1}, x_{e2}, \ldots, x_{en}) * \Delta x_j \\
&\qquad + \sum_{k=1}^{n}\left[\sum_{j=1}^{n} \left.\frac{\partial B_{i,j}}{\partial x_k}\right|_{x=x_e} \Delta x_k x_{ej}\right] + \sum_{k=1}^{n}\left[\sum_{j=1}^{n} \left.\frac{\partial B_{i,j}}{\partial x_k}\right|_{x=x_e} \Delta x_k \Delta x_j\right] \\
&\quad \cong \sum_{j=1}^{n} B_{i,j}(x_{e1}, x_{e2}, \ldots, x_{en}) * x_{ej} + \sum_{j=1}^{n} B_{i,j}(x_{e1}, x_{e2}, \ldots, x_{en}) * \Delta x_j \\
&\qquad + \sum_{k=1}^{n}\left[\sum_{j=1}^{n} \left.\frac{\partial B_{i,j}}{\partial x_k}\right|_{x=x_e} x_{ej}\right] \Delta x_k,
\end{aligned} \tag{39}$$

where the higher order term $\sum_{k=1}^{n}[\sum_{j=1}^{n} \partial B_{i,j}/\partial x_k|_{x=x_e}\, \Delta x_k \Delta x_j]$ has been neglected.

A more detailed expression for the last term of equation (41) can be obtained:

$$\sum_{k=1}^{n}\left[\sum_{j=1}^{n}\left.\frac{\partial B_{i,j}}{\partial x_k}\right|_{x=x_e} x_{ej}\right]\Delta x_k = \left[\sum_{j=1}^{n}\left.\frac{\partial B_{i,j}}{\partial x_1}\right|_{x=x_e} x_{ej} \cdots \sum_{j=1}^{n}\left.\frac{\partial B_{i,j}}{\partial x_n}\right|_{x=x_e} x_{ej}\right]\begin{bmatrix}\Delta x_1\\ \cdots\\ \Delta x_n\end{bmatrix}$$

$$= \left[\left[\frac{\partial B_{i,1}}{\partial x_1} \quad \cdots \quad \frac{\partial B_{i,n}}{\partial x_1}\right]_{x=x_e}\begin{bmatrix}x_{e1}\\ \cdots\\ x_{en}\end{bmatrix} \cdots \left[\frac{\partial B_{i,1}}{\partial x_n} \quad \cdots \quad \frac{\partial B_{i,n}}{\partial x_n}\right]\begin{bmatrix}x_{e1}\\ \cdots\\ x_{en}\end{bmatrix}_{x=x_e}\right]\begin{bmatrix}\Delta x_1\\ \cdots\\ \Delta x_n\end{bmatrix}$$

$$= \left[\left[\left[\frac{\partial B_{i,1}}{\partial x_1} \quad \cdots \quad \frac{\partial B_{i,n}}{\partial x_1}\right] \cdots \left[\frac{\partial B_{i,1}}{\partial x_n} \quad \cdots \quad \frac{\partial B_{i,n}}{\partial x_n}\right]\right]_{x=x_e} \otimes \begin{bmatrix}x_{e1}\\ \cdots\\ x_{en}\end{bmatrix}\right]\begin{bmatrix}\Delta x_1\\ \cdots\\ \Delta x_n\end{bmatrix}. \tag{40}$$

In the same way, for the second term on the right-hand side of equation (37), one obtains

$$\sum_{z=1}^{m} C_{1,z}(x_{e1}+\Delta x_1, x_{e2}+\Delta x_2, \ldots, x_{en}+\Delta x_n)*(v_{ez}+\Delta v_z)$$

$$= \sum_{z=1}^{m} C_{1,z}(x_{e1}, x_{e2}, \ldots, x_{en})*v_{ez} + \sum_{z=1}^{m} C_{1,z}(x_{e1}, x_{e2}, \ldots, x_{en})*\Delta v_z$$

$$+ \sum_{k=1}^{n}\left[\sum_{z=1}^{m}\left.\frac{\partial C_{i,z}}{\partial x_k}\right|_{x=x_e}\Delta x_k v_{ez}\right] + \sum_{k=1}^{n}\left[\sum_{z=1}^{n}\left.\frac{\partial C_{i,z}}{\partial x_k}\right|_{x=x_e}\Delta x_k \Delta v_z\right]$$

$$\cong \sum_{j=1}^{n} C_{i,z}(x_{e1}, x_{e2}, \ldots, x_{en})*v_{ez} + \sum_{z=1}^{m} C_{i,j}(x_{e1}, x_{e2}, \ldots, x_{en})*\Delta v_z$$

$$+ \sum_{k=1}^{m}\left[\sum_{z=1}^{m}\left.\frac{\partial C_{i,z}}{\partial x_k}\right|_{x=x_e} v_{ez}\right]\Delta x_k, \tag{41}$$

where the higher order term $\sum_{k=1}^{n}[\sum_{z=1}^{m}\partial C_{i,z}/\partial x_k|_{x=x_e}\Delta x_k \Delta v_z]$ has been neglected.

A more detailed expression for the last term of equation (41) can be obtained:

$$\sum_{k=1}^{n}\left[\sum_{z=1}^{m}\left.\frac{\partial C_{i,z}}{\partial x_k}\right|_{x=x_e} v_{ez}\right]\Delta x_k = \left[\sum_{z=1}^{m}\left.\frac{\partial C_{i,z}}{\partial x_1}\right|_{x=x_e} v_{ez} \cdots \sum_{z=1}^{m}\left.\frac{\partial C_{i,z}}{\partial x_n}\right|_{x=x_e} v_{ez}\right]\begin{bmatrix}\Delta x_1\\ \cdots\\ \Delta x_n\end{bmatrix}$$

$$= \left[\left[\frac{\partial C_{i,1}}{\partial x_1} \cdots \frac{\partial C_{i,m}}{\partial x_1}\right]_{x=x_e}\begin{bmatrix}v_{e1}\\ \cdots\\ v_{em}\end{bmatrix} \cdots \left[\frac{\partial C_{i,1}}{\partial x_n} \cdots \frac{\partial C_{i,m}}{\partial x_n}\right]_{x=x_e}\begin{bmatrix}v_{e_1}\\ \cdots\\ v_{em}\end{bmatrix}\right]\begin{bmatrix}\Delta x_1\\ \cdots\\ \Delta x_n\end{bmatrix}$$

$$= \left[\left[\left[\frac{\partial C_{i,1}}{\partial x_1} \cdots \frac{\partial C_{i,m}}{\partial x_1}\right] \cdots \left[\frac{\partial C_{i,1}}{\partial x_n} \cdots \frac{\partial C_{i,m}}{\partial x_n}\right]\right]_{x=x_e} \otimes \begin{bmatrix}v_{e_1}\\ \cdots\\ v_{em}\end{bmatrix}\right]\begin{bmatrix}\Delta x_1\\ \cdots\\ \Delta x_n\end{bmatrix}. \tag{42}$$

With respect to the above equations, it should be noted that the "$\otimes$" symbol is meant to indicate the inner product of the vectors

$$\left[\frac{\partial B_{i,1}}{\partial x_j} \cdots \frac{\partial B_{i,n}}{\partial x_j}\right]_{x = x_e} \quad \text{and} \quad \left[\frac{\partial C_{i,1}}{\partial x_j} \cdots \frac{\partial C_{i,n}}{\partial x_j}\right]_{x = x_e},$$

respectively (for any $i$ and $j$), by the vectors $\mathbf{x}_e$ and $\mathbf{v}_e$.

Then, by considering all the system rows, for the two sides of equation (37), one obtains:

$$\mathbf{A}(\mathbf{x}_e + \Delta\mathbf{x}(t))\,\Delta\dot{\mathbf{x}}(t) \cong \mathbf{A}(\mathbf{x}_e)\,\Delta\dot{\mathbf{x}}(t), \tag{43}$$

$$\begin{aligned}\mathbf{B}(\mathbf{x}_e + \Delta\mathbf{x}(t))\cdot(\mathbf{x}_e + \Delta\mathbf{x}(t)) + \mathbf{C}(\mathbf{x}_e + \Delta\mathbf{x}(t))\cdot(\mathbf{v}_e + \Delta\mathbf{v}(t)) \\ = \mathbf{B}(\mathbf{x}_e)\mathbf{x}_e + \mathbf{C}(\mathbf{x}_e)\mathbf{v}_e + \left[\mathbf{B}(\mathbf{x}_e) + \left(\left.\frac{\partial \mathbf{B}}{\partial \mathbf{x}}\right|_{\mathbf{x} = \mathbf{x}_e} \otimes \mathbf{x}_e\right) + \left(\left.\frac{\partial \mathbf{C}}{\partial \mathbf{x}}\right|_{\mathbf{x} = \mathbf{x}_e} \otimes \mathbf{v}_e\right)\right] \\ \Delta\mathbf{x}(t) + \mathbf{C}(\mathbf{x}_e)\Delta\mathbf{v}(t).\end{aligned} \tag{44}$$

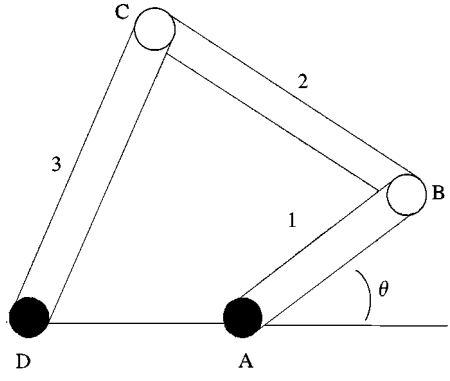


Figure 2. The four-link flexible mechanism to which the model has been applied.

TABLE 1

*Kinematic and dynamic features of the mechanism under investigation*

| Link lengths | | | |
|---|---|---|---|
| AB | BC | CD | DA (fixed frame) |
| 0·360 m | 0·528 m | 0·636 m | 0·332 m |

Square 6 mm × 6 mm cross-section; linearly distributed mass of the links = 0·272 kg m; flexural stiffness $EJ = 20{\cdot}142\ \mathrm{N\,m^2}$.

| Concentrated masses and inertias | | | |
|---|---|---|---|
| Joint A (inertia) | Joint B (mass) | Joint C (mass) | Joint D (inertia) |
| $3{\cdot}971 \times 10^{-4}\ \mathrm{kg\,m^2}$ | 0·040 kg | 0·040 kg | $1{\cdot}656 \times 10^{-4}\ \mathrm{kg\,m^2}$ |

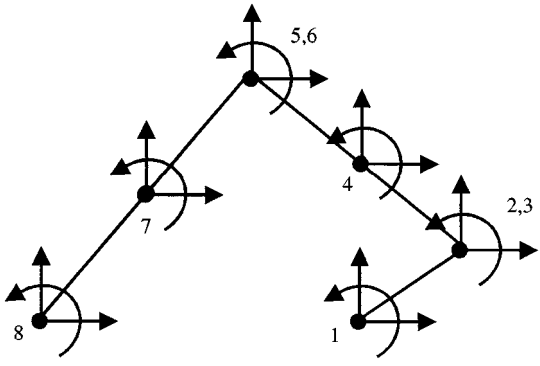


Figure 3. Location of the nodes and elastic translations and rotation associated with each node.

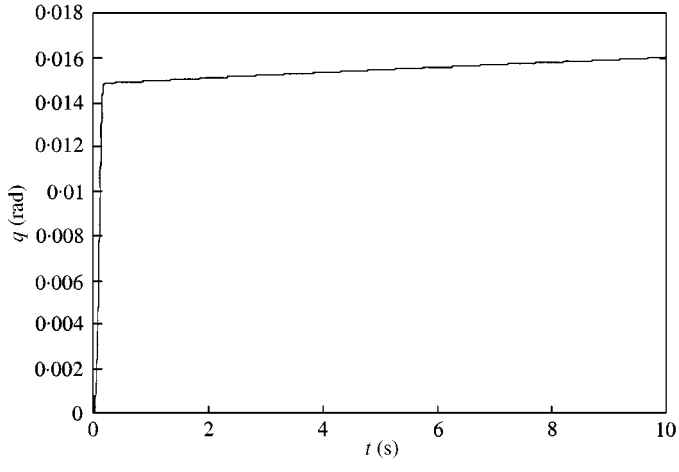


Figure 4. Response of the linearized system in open-loop conditions and without gravity.

Upon recalling that, according to the definition of the equilibrium point

$$\mathbf{B}(\mathbf{x}_e)\mathbf{x}_e + \mathbf{C}(\mathbf{x}_e)\mathbf{v}_e = \mathbf{A}(\mathbf{x}_e)\dot{\mathbf{x}}_e = \mathbf{0}, \tag{45}$$

the system linearized about an operating point can be written as

$$\mathbf{A}(\mathbf{x}_e)\Delta\dot{\mathbf{x}}(t) = \left[\mathbf{B}(\mathbf{x}_e) + \left(\frac{\partial \mathbf{B}}{\partial \mathbf{x}}\bigg|_{\mathbf{x}=\mathbf{x}_e} \otimes \mathbf{x}_e\right) + \left(\frac{\partial \mathbf{C}}{\partial \mathbf{x}}\bigg|_{\mathbf{x}=\mathbf{x}_e} \otimes \mathbf{v}_e\right)\right]\Delta\mathbf{x}(t) + \mathbf{C}(\mathbf{x}_e)\Delta\mathbf{v}(t). \tag{46}$$

Once the operating point $\mathbf{x}_e$ is set, the computation of the matrices $\mathbf{A}(\mathbf{x}_e)$, $\mathbf{B}(\mathbf{x}_e)$ and $\mathbf{C}(\mathbf{x}_e)$ is straightforward, and the matrices

$$\left(\frac{\partial \mathbf{B}}{\partial \mathbf{x}}\bigg|_{\mathbf{x}=\mathbf{x}_e} \otimes \mathbf{x}_e\right) \quad \text{and} \quad \left(\frac{\partial \mathbf{C}}{\partial \mathbf{x}}\bigg|_{\mathbf{x}=\mathbf{x}_e} \otimes \mathbf{v}_e\right)$$

can be determined according to their definitions, given by equations (40) and (42).

Now the matrices appearing in the above equation are constant; therefore, the system (46) can be written in a more compact form,

$$\mathbf{A}\Delta\dot{\mathbf{x}}(t) = \mathbf{B}\Delta\mathbf{x}(t) + \mathbf{C}\Delta\mathbf{v}(t), \tag{47}$$

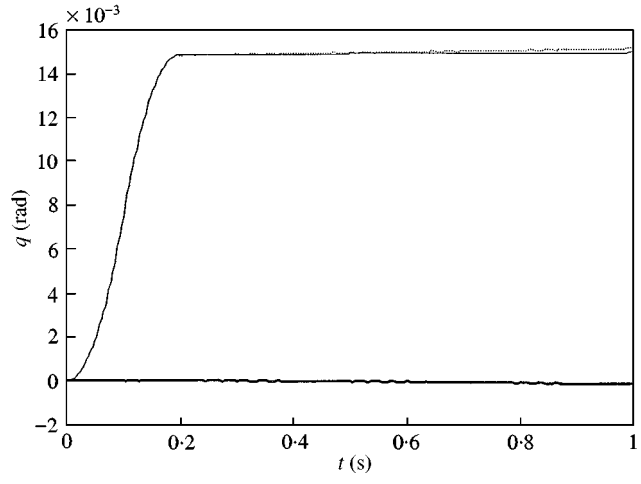


Figure 5. Comparison between the non-linear system and the linearized one in open-loop conditions without gravity: (⋯ ⋯), non-linear system; (——), linearized system; (——), error.

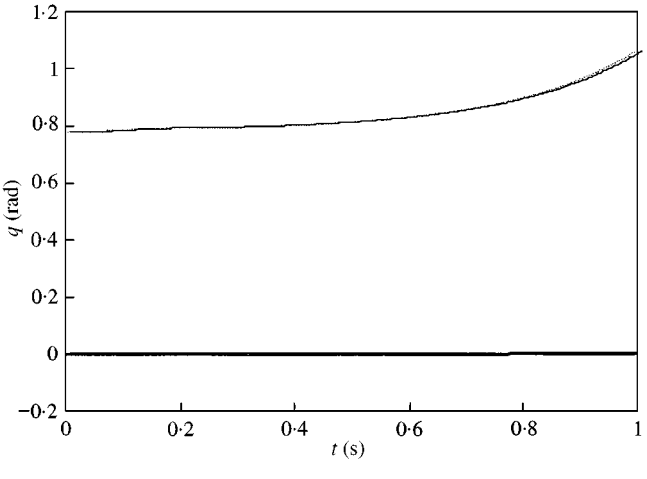


Figure 6. Comparison between the non-linear system and the linearized one in open-loop conditions with gravity. (⋯ ⋯), non-linear system; (——), linearized system; (——), error.

where the matrices **A**, **B** and **C** are constant matrices that are defined accordingly. Hence, it can be stated that the system (36) has been linearized.

## 4. APPLICATION OF THE MODEL TO A SPECIFIC CASE: A FLEXIBLE FOUR-LINK PLANAR MECHANISM

The model presented in the previous sections is valid for whatever planar mechanism with any number of free coordinates: In order to get some simulation results, one particular mechanism has been chosen, namely a four-bar mechanism with flexible steel links, and the model has been particularized to this case.

Figure 2 shows the particular mechanism under investigation. The kinematic and dynamic characteristics of that mechanism are reported in Table 1.

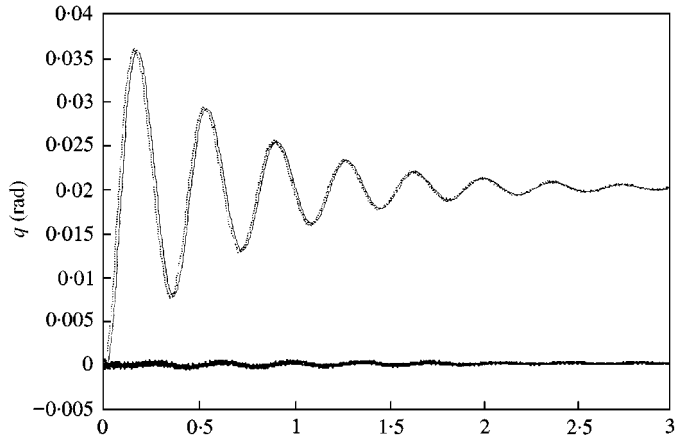


Figure 7. Comparison between the non-linear system and the linearized one in closed-loop conditions without gravity. Operating point: $q = 0$ rad; Kp = 10·0, Ki = 0·0, Kd = 0·1. (⋯ ⋯), non-linear system; (——), linearized system; (——), error.

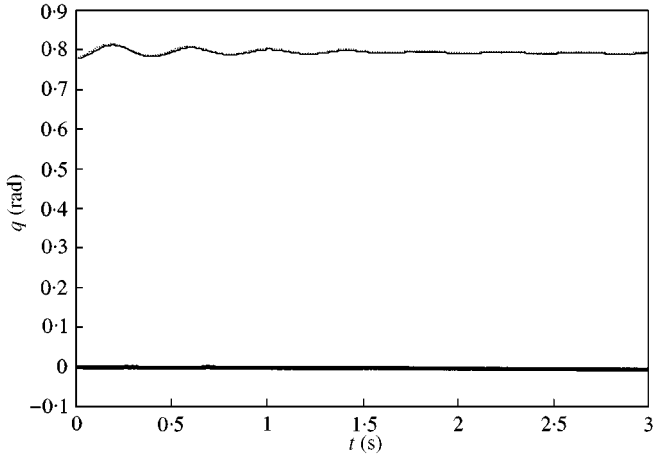


Figure 8. Comparison between the non-linear system and the linearized one in closed-loop conditions without gravity. Operating point: $q = 0{\cdot}78$ rad; Kp = 10·0, Ki = 1·0, Kd = 0·1. (⋯ ⋯), non-linear system; (—), linearized system; (—), error.

In order to apply the model described in the previous sections, a certain number of nodes must be chosen. Eight nodes have been defined, namely one at each link extremity and one at the midpoints of links 2 and 3. The locations of the eight nodes are shown in Figure 3. Hence, link 1 is modelled as a single beam element, links 2 and 3 are modelled as two beam elements each.

Thus, the mechanism under investigation has 24 elastic degrees of freedom (two translations in the $X$ and $Y$ directions and a rotation about the $Z$-axis for each node) and one degree of freedom (the crank angle) of the associated ERLS (see Figure 3). Of course, some of the elastic degrees of freedom are "fake", because the translations of the two revolute joints connected to the frame are to be zeroed, and the translations of the nodes lying at the same revolute joint should be equated. With reference to Figure 3, and letting

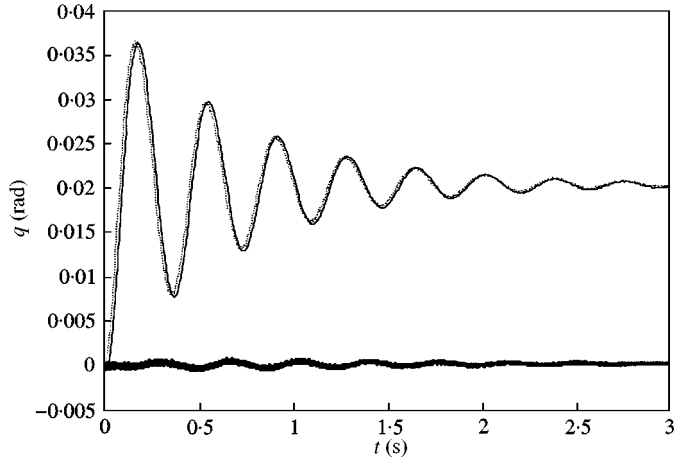


Figure 9. Comparison between the non-linear system and the linearized one in closed-loop conditions without gravity. Operating point: $q = 0$ rad; Kp = 10·0, Ki = 0·0; Kd = 0·1. (⋯ ⋯), non-linear system; (——), linearized system; (——), error.

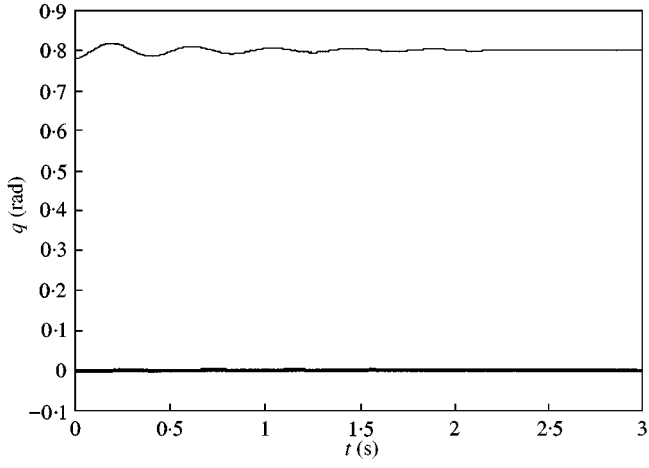


Figure 10. Comparison between the non-linear system and the linearized one in closed-loop conditions with gravity. Operating point: $q = 0{\cdot}78$ rad; Kp = 10·0, Ki = 1·0, Kd = 0·1. (⋯ ⋯), non-linear system; (——), linearized system; (——), error.

$s_x(i)$ and $s_y(i)$ denote the $X$ and $Y$ displacements of the $i$th node, it should be considered that,

$$s_x(1) = s_y(1) = 0, \quad s_x(8) = s_y(8) = 0, \quad s_x(2) = s_x(3),$$

$$s_y(2) = s_y(3), \quad s_x(5) = s_x(6), \quad s_y(5) = s_y(6).$$

Moreover, as explained in the previous section, the value of the elastic displacement of one among the remaining elastic degrees of freedom must be imposed, in order to correctly define the ERLS. In this case, it was chosen to equate to zero the $X$ translation of the point $C$: $s_x(5) = s_x(6) = 0$.

Once these considerations have been done, the linearized dynamic model presented in the foregoing, which is valid for any planar mechanism, can be applied to this particular mechanism.

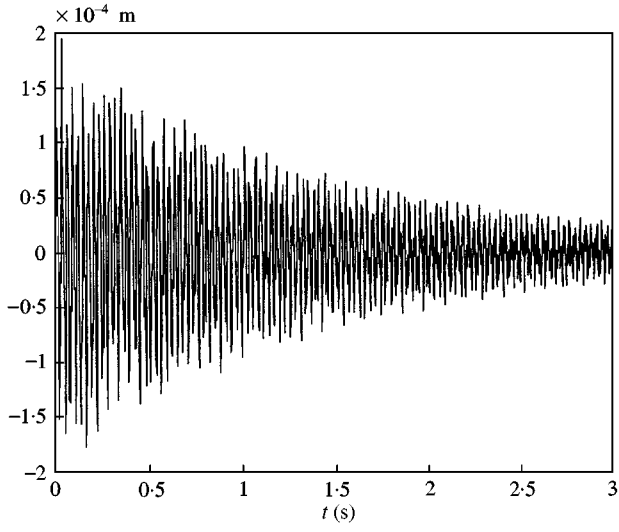


Figure 11. Horizontal (along the $X$ direction) elastic displacement of the midspan of link 3 (node 7) according to the non-linear model.

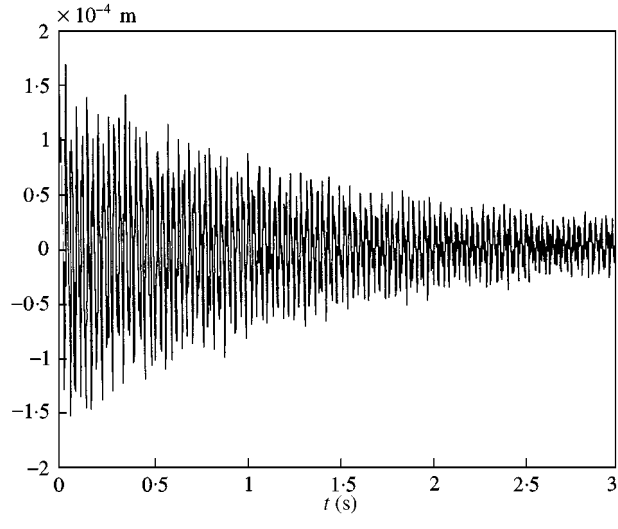


Figure 12. Horizontal (along the $X$ direction) elastic displacement of the midspan of link 3 (node 7) according to the linearized model.

## 5. COMPARISON BETWEEN THE LINEARIZED MODEL AND THE NON-LINEAR ONE

In order to prove the validity of the linearized model, several tests have been carried out, consisting in simulating the behaviour of the system using the non-linear model and comparing it with the results obtained by using the linearized model. In this way the range of validity of the linearization, namely the interval about the operating point for which the linearization holds, can also be found. Two types of tests have been done, namely, open- and closed-loop tests, using a classic PID compensator. In both cases the results have been good, showing that the linearization about an operating point yields a good approximation of the original non-linear system. This allows to state that the linearized model presented in

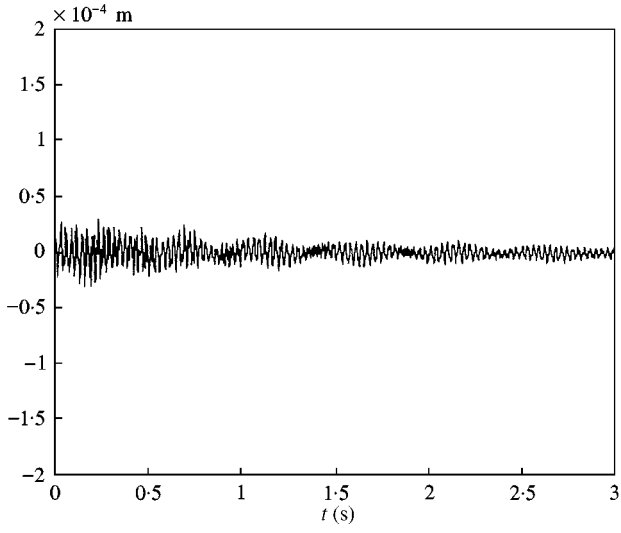


Figure 13. Error between the non-linear and the linearized model for the horizontal (along the $X$ direction) elastic displacement of the midspan of link 3 (node 7).

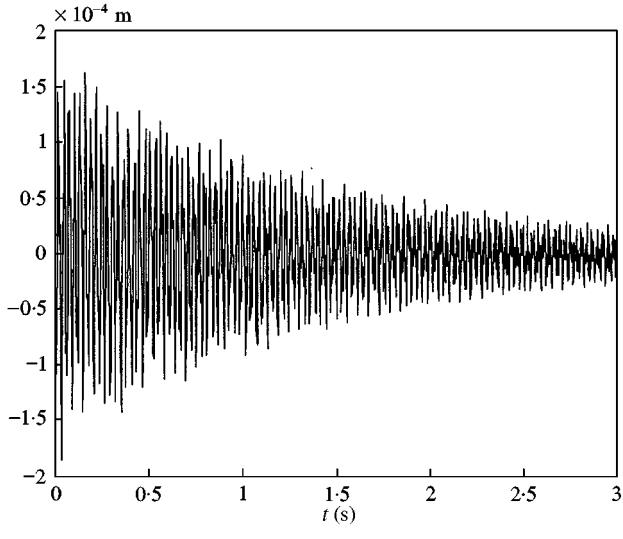


Figure 14. Vertical (along the $Y$ direction) elastic displacement of the midspan of link 3 (node 7) according to the non-linear model.

this work is an effective tool to be used to design and test any vibration controller for a planar flexible mechanism.

### 5.1. OPEN-LOOP TESTS

The tests consisted in evaluating the response of the flexible four-bar planar linkage described in the previous section to the following torque input: $\tau = 0{\cdot}05$ N m, $0 < t < 0{\cdot}1$ s; $\tau = -0{\cdot}05$ N m, $0{\cdot}1$ s $< t < 0{\cdot}2$ s; $\tau = 0$, $t < 0$ and $> 0{\cdot}2$ s.

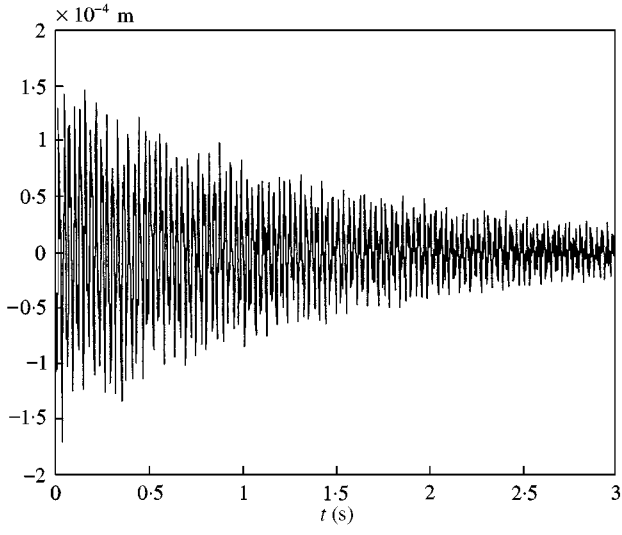


Figure 15. Vertical (along the $Y$ direction) elastic displacement of the midspan of link 3 (node 7) according to the linearized model.

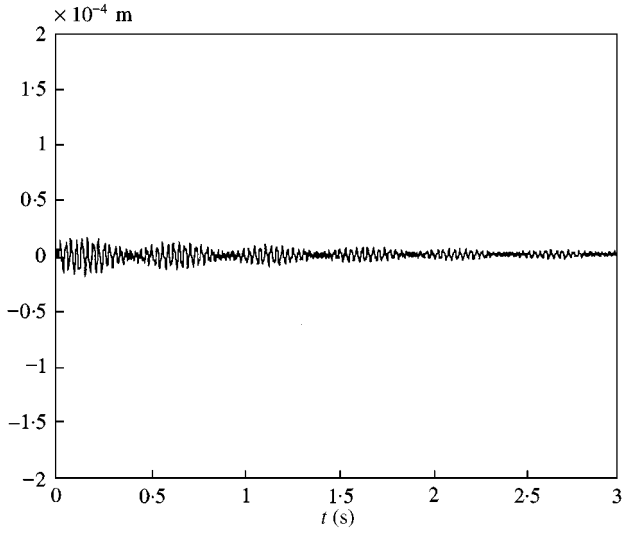


Figure 16. Error between the non-linear and the linearized model for the vertical (along the $Y$ direction) elastic displacement of the midspan of link 3 (node 7).

The first test with this input was done without including the gravity force in the model (i.e., considering the mechanism moving in a horizontal plane) and taking $q = 0$ as the operating point. The results of this test are shown in Figure 4.

In order to verify the validity of the linearization, the same input has been applied to the non-linear system, and the results have been compared with the previous ones. As shown in Figure 5, both models have a divergent response, and the correspondence between the two responses is very good. Further tests have been carried out including the gravity force in the model: Figure 6 shows the comparison between the response of the linearized system and that of the non-linear one. The linearization has been done about the configuration:

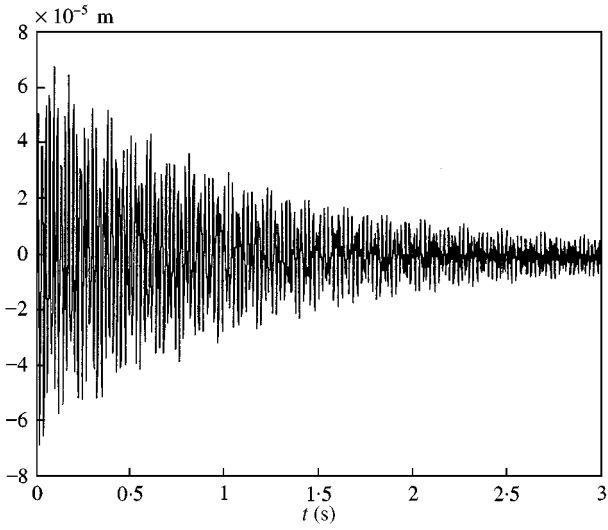


Figure 17. Horizontal (along the $X$ direction) elastic displacement of the midspan of link 2 (node 4) according to the non-linear model.

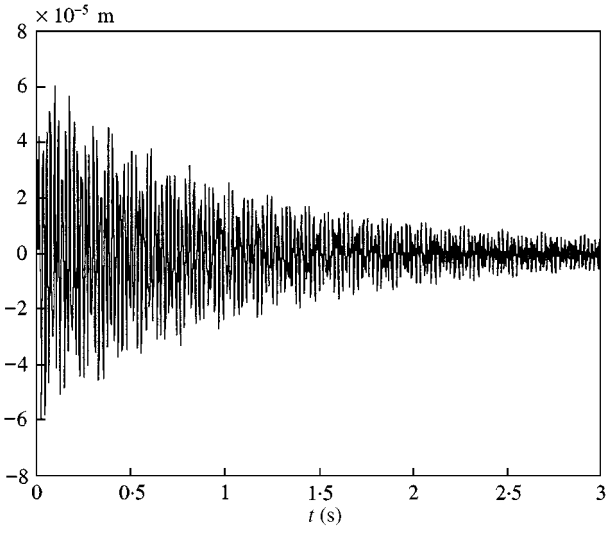


Figure 18. Horizontal (along the $X$ direction) elastic displacement of the midspan of link 2 (node 4) according to the linearized model.

$q = 0{\cdot}78$ rad. Again, the correspondence between the linearized model and the non-linear one is very good, and the error keeps very small.

## 5.2. CLOSED-LOOP TESTS

Further tests have been carried out, with the system inserted in a feedback loop with a classical PID regulator. A step of the free coordinate with amplitude $\Delta q = 0{\cdot}02$ rad has been input to the closed-loop system. The results of the tests for two different operating

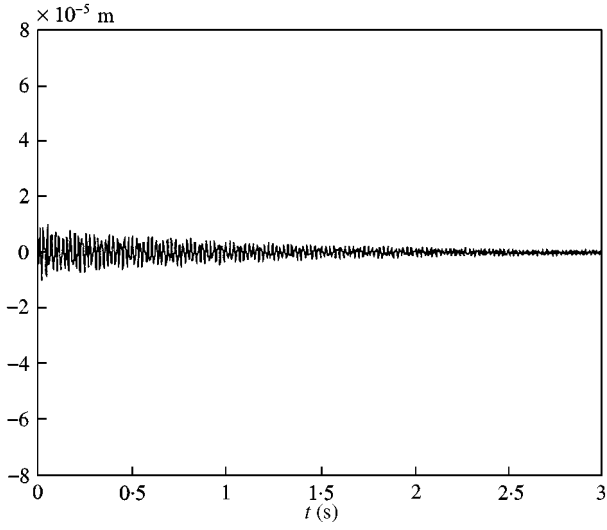


Figure 19. Error between the non-linear and the linearized model for the horizontal (along the $X$ direction) elastic displacement of the midspan of link 2 (node 4).

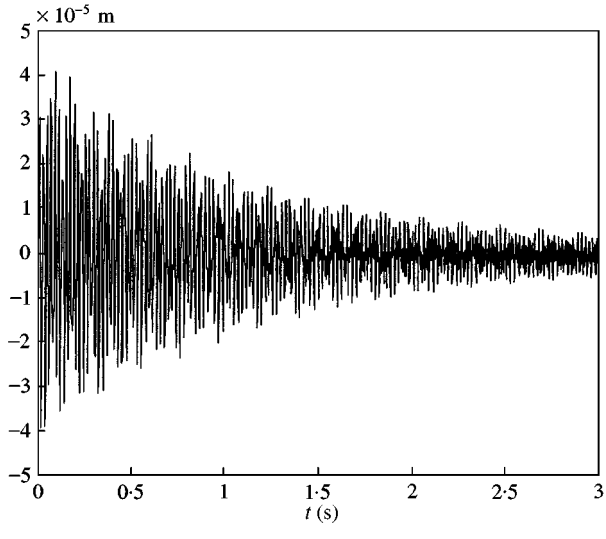


Figure 20. Vertical (along the $Y$ direction) elastic displacement of the midspan of link 2 (node 4) according to the non-linear model.

positions, namely $q = 0$ and 0·78 are presented here. Figures 7 and 8 show the results without including the gravity force in the model, whereas Figures 9 and 10 show the results obtained including the gravity force in the model. It can be noted that, in all cases, the behaviour of the linearized system is in good correspondence with that of the non-linear one. The error is very small (less than 1%) and its tiny fluctuations are given more by the fact that the response of the linearized system is slightly in advance with respect to that of the non-linear one, rather than a real difference in the amplitude of the response.

Further tests have been carried out, regarding the nodal elastic displacements generated by a step of the free co-ordinate of 0·02 rad. Figures 11 and 12 show the $X$ elastic

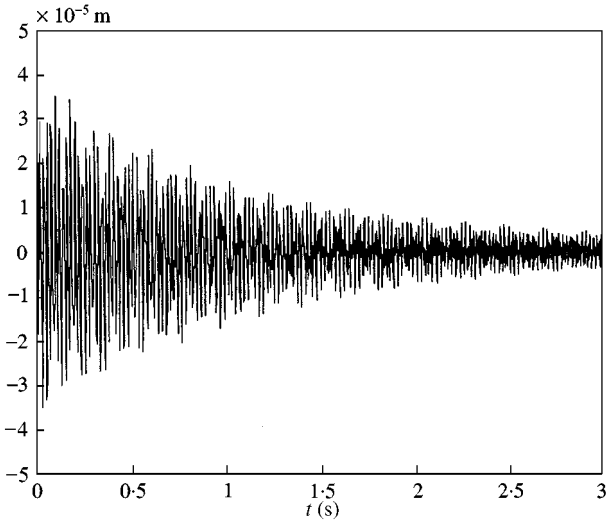


Figure 21. Vertical (along the $Y$ direction) elastic displacement of the midspan of link 2 (node 4) according to the linearized model.

displacement of node 7 (at the midspan of link 3), according to the non-linear and to the linearized model, respectively. Figure 13 shows the corresponding error. Figures 14 and 15 show the $Y$ elastic displacement of node 7 (at the midspan of link 3), according to the non-linear and to the linearized model respectively. Figure 16 shows the corresponding error. Figures 17 and 18 show the $X$ elastic displacement of node 4 (at the midspan of link 2), according to the non-linear and to the linearized model respectively. Figure 19 shows the corresponding error. Figures 20 and 21 show the $Y$ elastic displacement of node 4 (at the midspan of link 2), according to the non-linear and to the linearized model respectively. Figure 22 shows the corresponding error. It can be noticed that the amplitude of the error generated by the linearization keeps small, although the elastic nodal displacement is very little in amplitude and has several high-frequency components.

Furthermore, since for any linearization the field of validity of the linearized model is restricted to a certain interval centered at the operating point for which the linearization is performed, some tests have been carried out in order to determine the amplitude of the interval about the operating point for which the linearization yields a good enough approximation of the non-linear model. The tests have been carried out for the system in closed-loop conditions and with increasing amplitudes of the step input given to the free co-ordinate (from $\Delta q = 0{\cdot}1$ to $0{\cdot}6$ rad). The results proved that the linearization is effective even for displacements of the free coordinate from the operating point up to $1{\cdot}2$ rad. In this case, the relative error at the steady state is smaller than 3%.

## 6. CONCLUSION

An accurate dynamic model of a flexible-link planar mechanism has been presented in this paper. The overall motion of the mechanism has been decomposed into the rigid motion of a suitably defined ERLS and an overlapped elastic motion. Then, the equations of motion for the flexible mechanism have been obtained by direct application of the virtual work principle. This yields the elastic accelerations of the nodes and the accelerations of the free co-ordinates of the mechanism, while the correspondent velocities and displacements are obtained by integration.

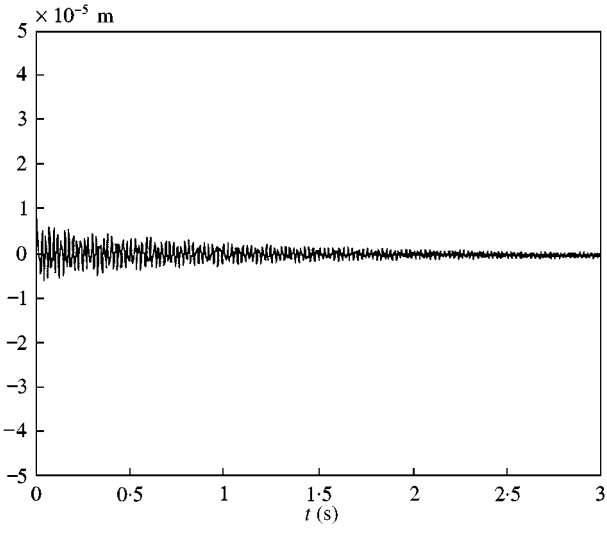


Figure 22. Error between the non-linear and linearized model for the horizontal (along the $Y$ direction) elastic displacement of the midspan of link 2 (node 4).

The dynamic model is strongly non-linear due to the quadratic relation between the nodal accelerations and the velocities of the free coordinates. Thus, it has been linearized about an operating point in order to get a model of the system in the state-space form.

The linearized model has then been applied to the case of a four-bar planar linkage. Several simulations have been carried out in order to prove the validity of the linearized model. The results show that the linearization is effective, i.e., the linearized model is a good representation of the non-linear one for an interval centered at the operating point, being the error introduced by the linearization very small both in open- and closed-loop systems.

It is believed that the linearized model proposed here can be a good base to implement and test different types of control for vibrations of flexible mechanisms.

## REFERENCES

1. G. G. Lowen and W. G. Jandrasits 1972 *Mechanism and Machine Theory* **7**, 3–17. Survey of investigation into the dynamic behaviour of mechanisms containing links with distributed mass and elasticity.
2. A. G. Erdman and G. N. Sandor 1972 *Mechanism and Machine Theory* **7**, 19–33. Kineto-elastodynamics—a review of the state-of-the-art and trends.
3. G. G. Lowen and C. C. Chassapis 1986 *Mechanism and Machine Theory* **21**, 33–42. The elastic behaviour of linkages: an update.
4. W. J. Book 1993 *ASME Journal of Dynamic Systems, Measurement and Control* **115**, 252–259. Controlled motion in an elastic world.
5. M. Giovagnoni and A. Rossi 1989 *Mechanism and Machine Theory* **24**, 231–243. Transient analysis of a flexible crank.
6. M. Giovagnoni 1993 *Journal of Sound and Vibration* **164**, 485–501. Linear decoupled models for a slewing beam undergoing large rotations.
7. S. P. Bhat, M. Tanaka and D. K. Miu 1991 *ASME Journal of Dynamic Systems, Measurement and Control* **113**, 432–443. Experiments on point-to-point position control of a flexible beam using Laplace transform technique—Parts I and II.
8. S. Cetinkunt and S. Wu 1992 *ASME Journal of Dynamic Systems, Measurement and Control* **114**, 428–435. Discrete-time tip position control of a flexible one arm robot.

9. D. S. KWON and W. J. BOOK 1994 *ASME Journal of Dynamic Systems, Measurement and Control* **116**, 193–200. A time-domain inverse dynamic tracking control of a single-link flexible manipulator.
10. R. H. CANNON and E. SCHMITZ 1984 *International Journal of Robotic Research* **3**, 62–75. Initial experiments on the end-point control of a flexible one-link robot.
11. A. A. GOLDENBERG and F. RASHKA 1986 *Mechanism and Machine Theory* **21**, 325–335. Feedforward control of a single-link flexible robot.
12. E. BARBIERI and Ü. ÖZGUNER 1988 *ASME Journal of Dynamic Systems, Measurement and Control* **110**, 416–421. Unconstrained and constrained mode expansions for a flexible slewing link.
13. A. SHCHUKA and A. A. GOLDENBERG 1989 *Mechanism and Machine Theory* **24**, 439–455. Tip control of a single-link flexible arm using a feedforward technique.
14. R. CARACCIOLO, E. CERESOLE and M. GIOVAGNONI 1996 *Journal of Robotics and Mechatronics* **8**, 112–121. Control experiment of a flexible robot arm using the floating frame model.
15. F. L. HU and A. G. ULSOY 1994 *ASME Journal of Dynamic Systems, Measurement and Control* **116**, 56–61. Dynamic modeling of constrained flexible robot arms for controller design.
16. B. SICILIANO, J. V. R. PRASAD and A. J. CALISE 1992 *ASME Journal of Dynamic Systems, Measurement and Control* **114**, 70–77. Output feedback two-time scale control of multilink flexible arms.
17. F. KHORRAMI and S. ZHENG 1992 *ASME Journal of Dynamic Systems, Measurement and Control* **114**, 580–585. An inner/outer loop controller for rigid–flexible manipulators.
18. A. S. YIGIT 1994 *ASME Journal of Dynamic Systems, Measurement and Control* **116**, 208–213. On the stability of PD control for a two-link rigid–flexible manipulator.
19. T. MERESSI and B. PADEN 1994 *Journal of Guidance, Control, and Dynamics* **17**, 537–544. Gain scheduled $H_\infty$ controllers for a two link flexible manipulator.
20. J. Z. XIA and C. H. MENQ 1993 *ASME Journal of Dynamic Systems, Measurement and Control* **115**, 385–392. Real time estimation of elastic deformation for end-point tracking control of flexible two-link manipulators.
21. R. I. MILFORD and S. F. ASOKANTHAN 1999 *Journal of Sound and Vibration* **222**, 191–207. Configuration dependent eigenfrequencies for a two-link flexible manipulator experiment verification.
22. S. NAGARAJAN and D. A. TURCIC 1990 *ASME Journal of Dynamic Systems, Measurement and Control* **112**, 203–214. Lagrangian formulation of the equations of motion for elastic mechanisms with mutual dependence between rigid body and elastic motions. Part I: element level equations.
23. S. NAGARAJAN and D. A. TURCIC 1990 *ASME Journal of Dynamic Systems, Measurement and Control* **112**, 215–224. Lagrangian formulation of the equations of motion for elastic mechanisms with mutual dependence between rigid body and elastic motions. Part II: systems equations.
24. L. MEIROVITCH and T. STEMPLE 1995 *Journal of Guidance, Control and Dynamics* **18**, 678–687. Hybrid equations of motion for flexible multibody systems using quasicoordinates.
25. J. LIEH 1994 *ASME Journal of Dynamic Systems, Measurement and Control* **116**, 702–709. Separated-form equations of motion of controlled flexible multibody systems.
26. K. H. YANG and Y. S. PARK 1996 *Mechanism and Machine Theory* **31**, 545–560. Dynamic stability analysis of a closed-loop flexible link mechanism.
27. M. KARKOUB and A. S. YIGIT 1999 *Journal of Sound and Vibration* **222**, 171–189. Vibration control of a four-bar mechanism with a flexible Coupler link.
28. D. A. TURCIC and A. MIDHA 1984 *ASME Journal of Dynamic Systems, Measurement and Control* **106**, 242–248. Generalized equations of motion for the dynamic analysis of elastic mechanism systems.
29. D. A. TURCIC and A. MIDHA 1984 *ASME Journal of Dynamic Systems, Measurement and Control* **106**, 249–254. Dynamic analysis of elastic mechanism systems. part I: applications.
30. D. A. TURCIC, A. MIDHA and J. R. BOSNIK 1984 *ASME Journal of Dynamic Systems, Measurement and Control* **106**, 255–260. Dynamic analysis of elastic mechanism systems. part II: experiment results.
31. L. W. CHANG and J. F. HAMILTON 1991 *ASME Journal of Dynamic Systems, Measurement and Control* **113**, 48–53. The kinematics of robotic manipulators with flexible links using an equivalent rigid link system (ERLS) model.
32. M. GIOVAGNONI 1994 *ASME Journal of Dynamic Systems, Measurement and Control* **116**, 73–80. A numerical and experimental analysis of a chain of flexible bodies.